الجمهورية الجزائرية الديمقراطية الشعبية
People's Democratic Republic of Algeria
وزارة التعليم العالي و البحث العلمي
Ministry of Higher Education and Scientific Research

المدرسة الوطنية العليا للتكنولوجيا و الهندسة - عنابة
National Higher School of Technology and Engineering – Annaba

Department of Process Engineering and Energetics

In Partial Fulfillment of the Requirements

for the Degree of
STATE ENGINEER

Field of Study: Energy and Sustainable Development

Presented by
BOULEGANE Yassmina
DAOUDI Ikram

Study of the Energy Performance of the Air Gas Production Unit at the Bellara Complex

Supervised by
Pr. AZZOUZ Salaheddine
ENSTI Annaba

Examination Board:

▪ MCA. BOUDINAR Naouam	President	ENSTI Annaba
▪ MCB. OTMANI Abdessalam	Examiner	ENSTI Annaba

Academic Year 2025

Acknowledgements

First of all, we are deeply grateful to God for His benevolence in making this graduation project possible.

We would like to take this opportunity to express our sincere thanks, especially to our dear parents and all the people who have provided their support, expertise and encouragement along the way.

We express our deepest gratitude to our dear supervisor, Professor Salah Eddine AZZOUZ, for his unwavering willingness to guide us. His availability and advices have been invaluable throughout this experience.

Dedication

As a token of our gratitude, we dedicate this modest work to all the people who have marked our academic and personal journey.

To ourselves. This project was the result of continuous cooperation, mutual support, and a combined effort. We are proud that this accomplishment is the product of a lovely and enduring partnership as well as a lot of hard work.

To our dear mothers for their patience, unconditional love, constant support and their unfailing encouragement, as well as for the sacrifices they made throughout our career, they were always a source of inspiration and motivation.

To our fathers who give us love, hope and strength.

To our friends for their friendship, moral support and moments of sharing. Thank you for the enriching discussions and the moments of conviviality.

To all those close to us and those we love.

Yassmina & Ikram

Abbreviations

Abbreviation	**Full Term / Description**
ASU	Air Separation Unit
HP	High Pressure (Distillation Column)
LP	Low Pressure (Distillation Column)
MAC	Main Air Compressor
MHE	Main Heat Exchanger
DCAC	Direct Cooling Air Contact
DCS	Distributed Control System
SEC	Specific Energy Consumption
LIN	Liquid Nitrogen
LOX	Liquid Oxygen
LAR	Liquid Argon
GAN	Gaseous Nitrogen
GOX	Gaseous Oxygen
GAR	Gaseous Argon
PRSV	Fluid Package in Aspen HYSYS

Nomenclature

Parameter	**Symbol**	**Unit**
Pressure	P	Kpa
Temperature	T	°C
Saturation Pressure	P_{sat}	Kpa
Specific Humidity	ω or e	kg H_2O / kg dry air
Electrical Power	$Q_{electric}$	kW or kWh
Useful Heat	Q_{useful}	kW
Work (Actual)	W_{actual}	kW
Work (Isentropic)	$W_{isentropic}$	kW
Enthalpy (Total)	H	kJ/h or kW
Enthalpy (Specific)	h	kJ/kg
ΔH (Total Enthalpy Change)	ΔH	kJ/h or MJ
Δh (Specific Enthalpy Change)	Δh	kJ/kg
Heat Transfer Rate (Real)	Q_{real}	kW
Heat Transfer Rate (Maximum)	Q_{max}	kW
Reboiler Duty	$Q_{reboiler}$	kW
Condenser Duty	$Q_{condenser}$	kW
Work by Booster Compressor	$W_{booster}$	kW
Work by Expander	$W_{expander}$	kW
Absorbed Power	$P_{absorbed}$	kW
Hydraulic Power	$P_{hydraulic}$	kW

Latent Heat of Vaporization	L_v	kJ/kg
Volumetric Flow Rate	Q	Nm^3/h
Mass Flow Rate	$\dot{m}$	kg/h
Molar Mass of Water Vapor	M_{H_2O}	18.015 g/mol (0.018015 kg/mol)
Molar Mass of Dry Air	M_{air}	28.97 g/mol (0.02897 kg/mol)
Specific Energy Consumption	SEC	KWh /kg or KWh /Nm^3

Abstract

The cryogenic air separation is a critical step in industrial applications requiring high-purity oxygen and nitrogen production such as steel making industries. This study focuses on evaluating the performance of the air separation unit located in Bellara, Jijel, using Aspen HYSYS V11 simulations, thermodynamic reference tables, and process flow diagrams.

Key performance indicators were established as follows: the separation efficiency was determined at 21.66%, within the expected range for double-column systems, while the overall efficiency was found to be 53%. The specific energy consumption for the total pure product was 0.47 kWh/kg, compared to 0.74 kWh/kg for high-purity oxygen.

Despite facing major challenges due to limited access to actual plant data, mainly due to confidentiality policies, the study successfully produced a technically reliable and insightful analysis. Importantly, the unit has not yet exhibited any significant degradation in performance, and the results obtained serve as proof of stable operation.

This study demonstrates that simulation and thermodynamic analysis can effectively uncover performance insights even when real data is incomplete.

Keywords*: Cryogenic air separation, separation efficiency, energy consumption, process simulation, thermodynamic analysis, Aspen HYSYS, heat loss, oxygen production.*

Résumé

La séparation cryogénique de l'air est une étape critique dans les applications industrielles nécessitant la production d'oxygène et d'azote de haute pureté, telles que les industries sidérurgiques. Cette étude se concentre sur l'évaluation des performances de l'unité de séparation d'air située à Bellara, Jijel, en utilisant des simulations Aspen HYSYS V11, des tables et des diagrammes thermodynamiques.

Les principaux indicateurs de performance ont été établis comme suit : l'efficacité de la séparation a été déterminée à 21,66 %, dans l'intervalle prévue pour les systèmes à double colonne, tandis que l'efficacité globale s'est avérée être de 53 %. La consommation d'énergie spécifique pour le produit pur total était de 0,47 kWh/kg, contre 0,74 kWh/kg pour l'oxygène de haute pureté.

Bien qu'elle ait été confrontée à des défis majeurs en raison de l'accès limité aux données réelles de l'usine, principalement en raison des politiques de confidentialité, l'étude a produit avec succès une analyse techniquement fiable et riche d'enseignements. Il est important de noter que l'unité n'a pas encore présenté de dégradation significative de ses performances et que les résultats obtenus sont la preuve d'un fonctionnement stable.

Cette étude démontre que la simulation et l'analyse thermodynamique peuvent efficacement mettre en évidence les performances même lorsque les données réelles sont incomplètes.

Mots-clés *: Séparation cryogénique de l'air, efficacité de séparation, consommation énergétique, simulation de procédé, analyse thermodynamique, Aspen HYSYS, pertes thermiques, production d'oxygène.*

الملخص

يُعد فصل الهواء بالتبريد خطوة مهمة في التطبيقات الصناعية التي تتطلب إنتاج الأكسجين والنيتروجين عالي النقاوة، مثل صناعة الصلب. تركز هذه الدراسة على تقييم أداء وحدة فصل الهواء الموجودة في بلارة بجيجل باستخدام المحاكاة باستعمال برنامج آسبن هايسيس والجداول والمخططات الديناميكية الحرارية.
وقد تم تحديد مؤشرات الأداء الرئيسية على النحو التالي: تم تحديد كفاءة الفصل بنسبة 21.66%، ضمن النطاق المتوقع لأنظمة الأعمدة المزدوجة، في حين تم تحديد الكفاءة الكلية بنسبة 53%. كان استهلاك الطاقة المحددة لإجمالي النواتج النقية 0.47 كيلو واط ساعة/كجم، مقارنة بـ 0.74 كيلو واط ساعة/كجم للأكسجين عالي النقاوة.

على الرغم من مواجهة تحديات كبيرة بسبب محدودية الوصول إلى بعض بيانات المصنع، إلا أن الدراسة نجحت في إنتاج تحليل سليم تقنيًا وغني بالمعلومات. والأهم من ذلك، نخص بالذكر ان الوحدة لم تظهر حتى الآن أي تدهور كبير في الأداء، والنتائج التي تم الحصول عليها دليل على استقرار التشغيل.
توضح هذه الدراسة أن المحاكاة والتحليل الديناميكي الحراري يمكن أن يسلط الضوء بشكل فعال على الأداء حتى عندما تكون البيانات الحقيقية غير مكتملة.

الكلما|1| الماح1ة اا : فصل الهواء بالتبريد، كفاءة الفصل، استهلاك الطاقة، محاكاة العملية، التحليل الديناميكي الحراري، الفاقد الحراري، إنتاج الأكسجين

Tables of content

CHAPTER I: AN OVERVIEW OF THE ALGERIAN QATARI STEEL COMPLEX.............

CHAPTER II: LITERATURE REVIEW...

CHAPTER III: PERFORMANCE CALCULATION OF EACH EQUIPMENT IN THE AIR SEPARATION UNIT (ASU)..

CHAPTER IV: RESULTS AND DISCUSSION...

GENERAL CONCLUSION ....

Tables list

Figure list

Introduction:

Algerian Qatari Steel is located in El-Milia wilaya of Jijel, where it operates a complex owned by Qatar Steel International (QSI) and the SIDER Industrial Group with a total area of 216 hectares in the industrial zone of Bellara is one of the pillars of industry in Algeria, with a capacity of four million tons of high-quality products in its four types: Cold direct reduction iron, billet, wire rods and reinforcing bars.

Manufacturing these final products from raw materials requires a series of related processes that take place in the various units of the factory which require high-purity gases represented by oxygen, nitrogen, and argon, which are obtained by separating atmospheric air into their basic components. Here lies the importance of the air separation unit, which ensures the continuous production of these gases through a process based on cryogenic distillation which operates at very low temperatures and high pressures.

The purpose of this final year project is to evaluate the performance of the unit based on the analysis of its key equipment that operates with a specific mass flow of atmospheric air under known conditions of pressure and temperature in order to determine all possible losses and identify the unit' efficiency.

Aspen HYSYS V11, a process simulation software that is widely recognized, has been utilized, confirmed by thermodynamic reference tables, and process flow diagrams.
The use of this tool allowed us to simulate and model the entire ASU process, which includes compression, cooling, purification, and cryogenic distillation, under realistic operating conditions.

This dissertation is organized into four chapters as follows:

- **Chapter 1** provides an overview of the Algerian Qatari Steel company, briefly describes the air separation plant and mentions the motivation and the problem statement.
- **Chapter 2**, titled *"Literature Review"*, summarizes previous research on air separation processes, including common issues that reduce efficiency and gas purity, as well as some proposed solutions and innovations.
- **Chapter 3** presents the mass and energy balances, besides the losses and efficiency for each piece of equipment, along with related calculations based on collected data and the results of the ASPEN HYSYS simulation.
- **Chapter 4** discusses the results obtained in Chapter 3, which form the basis for calculating key performance indicators used to assess the efficiency and performance of the Air Separation Unit.

Chapter I:

An overview of the Algerian Qatari Steel complex

Chapter I: An overview of the Algerian Qatari Steel complex

Introduction

This chapter is dedicated to the description of the air gas production process at the Algerian Qatari Steel complex (AQS) Bellara (Jijel), At the end of 2017, The Algerian Qatari steel company started the production and marketing of iron products by meeting the needs of the local iron market and by exporting surplus production to regional and international markets.

The Complex's initial production capacity is approximately 2 million tons per year of reinforcing bars and wire rods of various diameters. The second phase of the investment program will be dedicated to the production of other types of special steels used in many industries, thus bringing the production capacity to more than 4 million tons per year.

1.1 Structure of the complex:

The complex is structured to ensure efficient production and support operations. The principal production units comprise a Direct Reduced Iron (DRI) plant, a Steel Melt Shop (SMS), and three rolling mills. These are assisted by the main auxiliary units, such as a water treatment plant, a main receiving substation, a lime production plant, and an air separation unit, all integrated to enable sustained and optimized industrial operation.

1.2 Air separation unit description:

The ASU is often considered as the beating heart of the complex, using the Linde process, the ASU compresses, cools, and separates air into Oxygen, Nitrogen, and Argon through cryogenic distillation, it supplies pure oxygen, which is essential for key processes in the complex like fuel combustion in furnaces, iron production in the DRI process, and gas treatment.

The figure (1) describes the process of Air separation unit

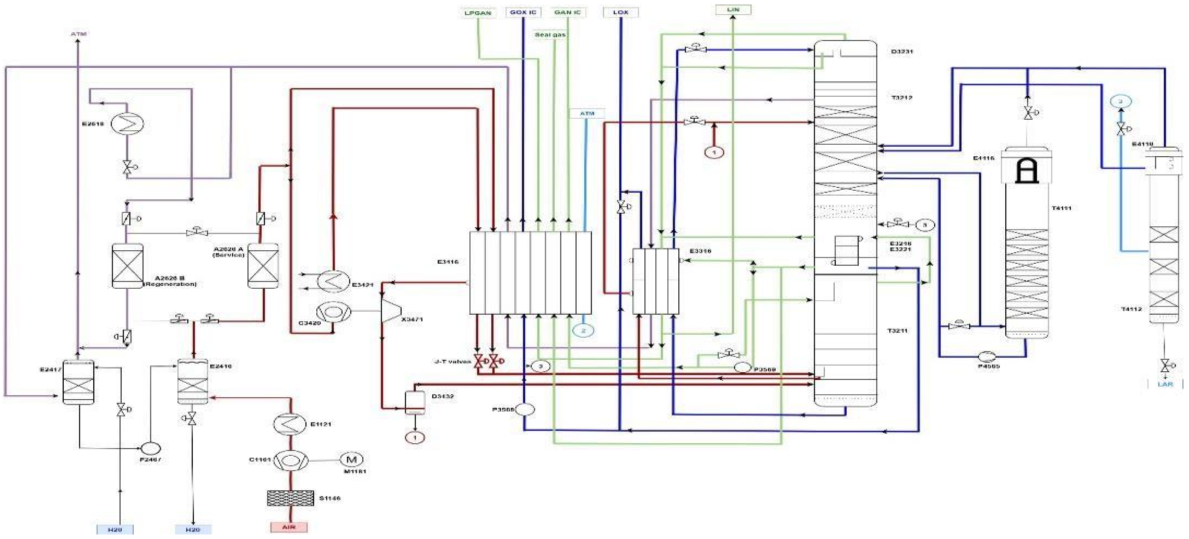

Figure 1 : Air separation unit Process

At flow rate of 115904 Nm^3/h, below in table (1), there is the difference theoretical end actual capacity that changes depending on the client's need.

Table 1 : Air separation unit Production

Production	theoretical capacity			Actual capacity		
	Gas (Nm3/h)	Liquid (m3/h)	Purity (%)	Gas (Nm3/h)	Liquid (m3/h)	Purity (%)
Oxygen	20450	1500	0,995	12452,93	2676,708	0,995
Nitrogen	9810	1500	0,999	9477,58	585,125	0,999
Argon	100	-	0,999	100	-	0,999

1.3 Air Separation Unit Process Description:

Air Filtration & Compression: Air is introduced under atmospheric conditions into a filter containing 140 cartridges (S1146) where solid and liquid impurities are removed.

The main air compressor (C1161), draws within the filtered air and compresses it to 22 bars through five stages, supported by four intercoolers and one aftercooler.

Air Cooling & Washing: The compressed air flows into the process air cooler (E2416), where it is cooled and washed so that harmful components (SO_2, SO_3, NH_3) are removed by direct contact with chilled water circulation ensured by pumps (P2467) from the evaporation cooler (E2418).

Purification: Residual moisture**,** CO_2**,** and hydrocarbons are further eliminated in the molecular sieve adsorbers, therefore to ensure the continuity of the operation, two vessels are required. One adsorber is in operation while the other is undergoing regeneration using the heated crude

Nitrogen taken from the distillation unit as a waste gas. This gas is heated up in the electrical regeneration gas heater (E2618) from about 10°C to about 225°C.

Refrigeration and air separation Cycle: A big portion of the purified air is compressed by a booster compressor (C3420), mechanically linked to the expansion turbine (X3471).to get cooled in the main heat exchanger (E3116), then be divided as follows:

One stream is liquefied in the heat exchanger, expanded via a Joule-Thomson (JT) valve, and fed into T3211 the distillation column.

And the second stream expands in the turbine X3471, generating refrigeration before entering the high-pressure column (T3211).

The cryogenic liquids are stored in six storage tanks with a capacity of 250 m^3 for each one.

1.4 Problem Statement

Air Separation Unit is mainly used to produce industrial high-purity gases. However, due to their complex process and limited access to operational data, evaluating their performance remains challenging.

This study seeks to answer: How can we evaluate the performance of this unit' component in a cryogenic air separation unit using theoretical analysis and process simulation to detect inefficiencies?

1.5 Motivation:

The performance evaluation of Air Separation Units (ASU) is crucial to understand their process, identify efficiency, losses and ensure the quality of the produced gases.

They include several key components such as compressors, Evaporation cooler, molecular sieves, heat exchangers, expander, and distillation columns. Analyzing each component, along with their interactions, helps assess the overall efficiency of the system.

using Aspen HYSYS, it is possible to simulate the real behavior of the ASU and track thermodynamic parameters in order to extract reliable performance indicators.

This evaluation allows to: Better understand the separation process, detect loss or inefficiency zones, support future technical decisions.

Chapter II:

Literature Review

Chapter II: Literature Review

Introduction:

Cryogenic air separation is an important industrial process used to generate gases such as oxygen, nitrogen and argon, which are used in metallurgy as well as chemical and energy production. While this process is effective, it requires a high amount of energy prompting industries to find ways to improve its efficiency. So, the study of Air Separation Units (ASUs) is fundamental to identify energy losses, suggest improvements, and lower operational costs.

In this last year project, the literature reviews is an essential part. It positions our study in the current scientific and technical framework, shows the advances and limitations of previous work, and provides rationale for the methodologies and technology employed. This paper aims to integrate the general trends in ASU research, critically analyze past contributions and their limitations, and open up directions for future inquiry that this paper tries to address.

2.1 Research Domain Description

The study is concerned with cryogenic air separation units. These units operate by liquefying the ambient air, then fractional distillation at very low temperatures to separate the various components of air based on their individual boiling points. A standard unit consists of a few major components: compressors, heat exchangers, distillation columns (low and high pressure), expansion turbines, and molecular sieves. The main concepts related to this domain include:

- Separation thermodynamics: energy balances, mass balances, liquid-vapor equilibrium. enthalpy-entropy diagram and thermodynamic table
- Exergy analysis: assessment of the quality of the energy consumed, determination of the sources of inefficiency.
- Energy integration: recycling of cold streams, heat exchange network optimization.
- Process modeling and simulation: Aspen HYSYS software is utilized for steady-state separation process modeling and simulation.

2.2 Previous Studies and Research

There have been numerous studies on the energy and exergy performance of air separation units (ASUs) with different aims from technological descriptions to high-level optimization.

Smith and Klosek's (2001)[1] paper is an extensive review of various air separation techniques with an emphasis on integration with other processes in the energy industry. The authors present the fundamental principles of cryogenic separation and provide additional possibilities using pressure swing adsorption and membrane permeation. The study gives a sound theoretical background for understanding the historical evolution and technological choice criteria according to industrial requirements.[1]

Sapali and Raibhole (2017) directed their study towards exergy analysis of an integrated into a biomass gasification plant. Through their study, it is evident how the qualitative study of energy in the components of the unit is significant. They were able to identify major zones of exergy destruction, especially in the distillation columns and heat exchangers, while suggesting theoretical changes for better overall efficiency[2].

Kumar (2014) studied the operation of a cryogenic air separation plant in a steel plant. The operation was simulated by the author under steady state along with an alternative based on fixed-bed adsorption being investigated, the study is very helpful in the context of understanding typical operating conditions in an industrial setup and the limitations in terms of purity of gases produced. The study, however, is restricted to a technical description without in-depth thermodynamic insight [3].

One more research, presented to the ICMERE conference (2015), deals with the reduction of energy consumption in ASUs by means of heat recovery and self-refrigeration. With its brevity, the research offers some possibilities for optimization of the overall ASU process and reduction of electrical power consumption[4] .

More recently, Bucsa et al. (2022) reported a comprehensive exergy analysis of an actual operating ASU. It relies on the quantification of exergy loss in each of the components, and it puts in perspective the leading role of exchangers and columns. [5]

Finally, Gürsoy et al. (2024) introduced an innovative approach founded on advanced exergy analysis. This approach elevates the internal loss quantification to another level by incorporating component interactions, technological constraints, and potential for improvement. This study is a major step forward in ASU performance diagnosis and optimization[6].

Previous works provide solid theoretical foundations and apply established methods like exergy analysis and simulation to analyze performance. They often combine several fields like thermodynamics, modeling, and optimization. Some also utilize actual data or experimental result, which make it more applicable to industry.

However, some of the studies are not validated experimentally to a satisfactory extent, which can make their results less reliable. The majority are based on idealized cases, which do not always reflect real industrial conditions, where operating conditions are non-constant. Few studies address the integration of air separation units with renewable or hybrid systems although it is an area that is growing at a rapid rate. Exergy analyses are often conducted on parts of the system alone, rather than the whole plant.

here is agreement on the significance of cryogenics as the main process for air separation and on the utilization of exergy to evaluate performance. However, optimization methods focus on technical improvements, the models are not all the same either; some include adsorption effects, while others do not.

These papers provide a good foundation for air separation unit modeling, simulation, and performance analysis. They show that combining that cryogenic simulation coupled with exergy analysis is a suitable approach for this project. It also counts to consider real operating conditions into consideration and include new developments to get more dependable and realistic results.

2.3 Conclusion:

This literature review was able to identify key developments in the field of air separation units, more particularly cryogenic-based approaches and exergy analysis. Previous research demonstrates the importance of these approaches in the optimization of energy and operational performance. However, some gaps remain, especially in terms of experimental validation and integration with modern hybrid systems.

The Final year project aims to address these deficiencies by proposing a particular model tested with real data, together with a comprehensive examination of energy integration, there by contributing to the optimization of the performance of the studied units.

Chapter III:

Performance Calculation of each equipment in the Air Separation Unit (ASU)

Chapter III: Performance Calculation of the Air Separation Unit (ASU)

Introduction:

The purpose of this final year project is to evaluate the performance of an Air Separation Unit (ASU) by analyzing its key components—namely the main air compressor, molecular sieves, expander, pumps, main heat exchangers, evaporation cooler, direct contact air cooler, and the distillation column—using tables, diagrams and Aspen HYSYS V11 simulation where the Peng- Peng-Robinson-Stryjek-Vera (PRSV) fluid package was selected, while we Take advantage of the calculation results to compare them with the unit's datasheets in order to evaluate the accuracy of the results obtained

We will begin by conducting losses, efficiencies, mass and energy balances for each piece of equipment within the ASU.

3.1 Energy and mass balances

The system operates with a specified flow rate of atmospheric air (115 904 Nm^3/h) under known pressure and temperature conditions. To start the analysis, we apply the fundamental principles of mass and energy balances to each component of the system.

The mass balance is represented by the equation (1):

$$\dot{m}_{in} = \dot{m}_{out} + \dot{m}_{losses} \qquad (1)$$

Similarly, the energy balance is expressed in the equation (2) :

$$H_{in} + Q = H_{out} + W \qquad (2)$$

Where: $$\Delta H = \dot{m}\, h_{out} - \dot{m}\, h_{in} \qquad (3) \qquad [kJ/h]$$

These equations will be systematically applied to each piece of equipment in the Air Separation Unit (ASU) in order to evaluate their individual performance.

3.1.1 Main air compressor C1161:

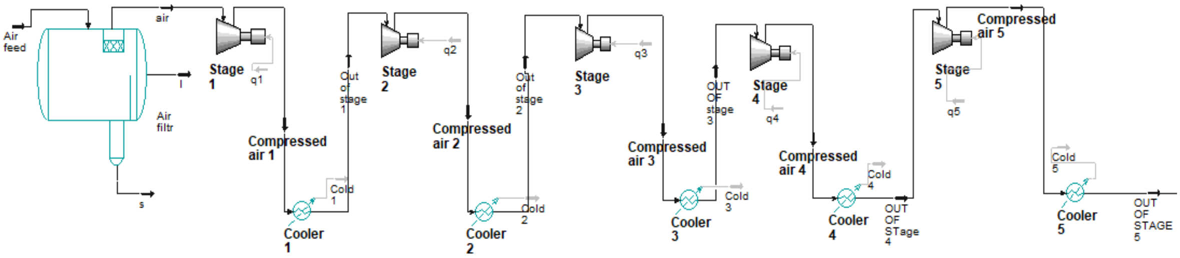

Figure 2 : Configuration of the Main air Compressor in Aspen HYSYS

- Masse balance:

The mass is conserved, with identical inlet and outlet flow rates of 1.497 × 10^5 kg/h, with no losses ($\dot{m}_{\text{losses}}$ = 0 Kg/h)

- Energy balance:

Using the data tables provided in the appendix, the saturated vapor pressure $P_S''(T)$ and specific humidity X [kg/kg] were determined for each compression stage [Table 19, Chapter 4], using the equation (4):

$$X_{\text{air}} = \frac{M_{H_2O}}{M_{\text{Dry\_air}}} \times \frac{e \times P''_v(T)}{P - e \times P''_v\ (T)} \qquad (4) \quad [\, Kg_{water\ vapor} / \, Kg_{Dry\ air}]$$

These values were used to calculate the inlet and outlet enthalpies using the equation (5):

$$h_{air} = C_{p,dry\ air} \times T + (X \times C_{p,v} * T) + X \times L_V \quad (5) \qquad [\text{KJ /kg}]$$

Where:

- $C_{p,dry\ air}$= 1.005 kJ/kg. K
- $C_{p,v}$=1.84 kJ/kg. K
- L_V= is the latent heat of vaporization, with values specified for each stage in the appendix [**Table Appendix 1**].

The results of these calculations are presented in [**Table 2],** which summarizes the enthalpy values, isentropic efficiencies, and energy losses for each stage.

Energy losses are defined as: Losses = $W_{\text{actual}} - W_{\text{is}}$

The isentropic efficiency of the main air compressor is calculated using the expression (6):

$$\eta_s = \frac{\text{Wis}}{\text{W actual}} = \frac{\dot{m} \times (\text{h2s} - \text{h1})}{\dot{m} \times (\text{h2} - \text{h1})} \qquad (6)$$

Table 2 : Efficiency and Losses Assessment in each stage [Main Air compressor]

Stage	h_{in} [kJ/kg]	h_{out} [kJ/kg]	Δh [kJ/kg]	W_{actual}	W_{is}	Efficiency (%)	Losses [Kw]
1	310.94	383.22	72.28	3006.43	2555.47	85%	450.96
2	645.59	734.17	88.58	3685.95	3133.06	85%	552.89
3	316.89	389.51	72.62	3023.35	2570.85	85%	452.50
4	312.74	384.92	72.18	3002.53	2552.15	85%	450.38

5	307.69	383.44	75.75	3148.34	2676.09	85%	472.25
Total	1893.85	2275.26	381.41	15866.6	13487.6	85%	2379

Table [3] presents a comparison between the theoretical values from the datasheet, the actual calculated results, and the simulation results obtained from Aspen HYSYS for the main air compressor

Table 3 : Comparison of the MAC Results

	Q [Nm^3/h]	**T_{in} [K]**	**T_{out} [K]**	**P_{in} |Pa] ×10^5**	**P_{out} [Pa] ×10^5**	**W_{actual} [kW]**	**Wis [KW]**	**ηs [%]**	**Losses [KW]**
Theoretical	115310	292	347	101.30	22 .25	14256	12212	85	2044
Actual 'analysis'	115904	286.1	375	100.20	20.66	15866.6	13487	85	2379
Actual 'Aspen hysys'	115904	286.1	375	100.20	20.66	13408,4	11399	85	2011,7

3.1.2 Direct Contact Air Cooling (DCAC) E2416:

The column is adiabatic (Q = 0) and has no chemical reactions, so the energy balance simply means that the total inlet enthalpy equals the total outlet enthalpy

- Masse balance:

The mass is conserved, with identical inlet and outlet flow rates

of 2.095 × 10^5 kg/h, and no mass losses observed ($\dot{m}_{losses}$ = 0 kg/h).

- Energy balance

– For the air:

The thermodynamic parameters used to calculate enthalpy are taken from the tables presented in the appendix.

($\dot{m}_{Air}$ dry =149541.47 kg/h)

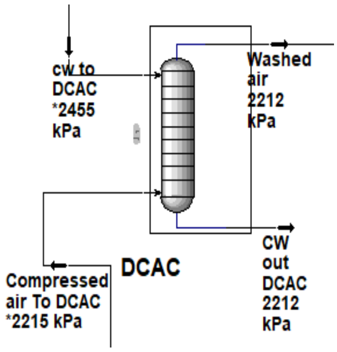

Figure 3 : Configuration of the DCAC in Aspen HYSYS

Table 4*: Thermodynamic Parameters of the air in the DCAC*

Stream	T [°C]	P [kPa]	P_{sat} [kPa]	x [$Kg_{water\ vapor}$/ $Kg_{Dry\ air}$]	h [kJ/kg]	Δh [kJ/kg]	ΔH [kJ/h]	ΔH [Kw]
Inlet	26.40	2215	4.066	0.001143	29.45	–17.57	–2,62×10^6	–729.7
Outlet	10.90	2212	1.303	0.000366	11.88			

- For water:

We use the equation (7) to calculate the enthalpy of water in the DCAC

$h_{\text{liquid}}(T) = Cp \times T$ (7)

Where $Cp = 4.18$ kJ/kg·°C & $\dot{m}_{\text{water}} = 50264.4$ kg/h

Table 5 : Thermodynamic Parameters of water in the DCAC

Stream	T [°C]	P [kPa]	h [kJ/kg]	Δh [kJ/kg]	ΔH [kJ/h]	ΔH [kW]
Inlet	10,70	2455	43.47	50.40	$-2{,}51\times10^{6}$	698.52
Outlet	10.90	2212	93.87			

The energy efficiency of the direct contact air cooling is expressed by the equation (8)[7] :

$$\eta = \frac{\text{Useful heat gained by water}}{\text{Heat lost by air}} \quad (8)$$

$$\eta = \frac{|\Delta H\text{water}|}{|\Delta H\text{air}|} = 0{,}957 = 95{,}7\%$$

Energy losses are expressed by the equation (9) :

$Q_{\text{loss}} = |\Delta H_{\text{air}}| - |\Delta H_{\text{water}}|$ (9)

$Q_{\text{loss}} = 729.7 - 698.52 = 40{,}18$ kw

Table 6 : Comparison of the DCAC results

	Stream	Δh [kJ/kg]	ΔH [kJ/h]	ΔH [Kw]	Losses [KW]
Actual 'analysis'	Air	–17.57	$-2{,}62\times10^{6}$	- 729.7	40,18
	Water	50.40	$-2{,}51\times10^{6}$	698.52	
Actual Aspen hysys	Air	–16,95	$-2{,}5388\times10^{6}$	- 705,23	1,14
	Water	48,58	$-2{,}5334\times10^{6}$	704,09	

The Direct Contact Air Cooling (DCAC) column demonstrates a high thermal efficiency **(~95.7%)**, meaning that most of the heat removed from the humid air is successfully transferred to the washing water.

3.1.3 Molecular sieve A2626:

The column has no chemical reactions, so the energy balance simply means that the total inlet enthalpy equals the total outlet enthalpy

- Masse balance:

  mass is conserved, with identical inlet and outlet flow rates of $1{,}947 \times 10^{5}$ kg/h, and no mass losses observed ($\dot{m}_{\text{losses}} = 0$ kg/h).

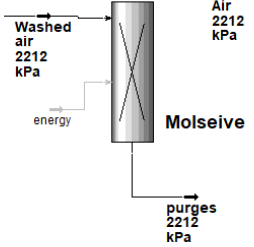

Figure 4 : Configuration of the Molseive in Aspen HYSYS

- Energy balance:

Table 7 : Energy balance in the Molseive

Stream	Mass Flow [kg/h]	h [kJ/kg]	H [kJ/h]	H [kW]
Inlet Washed Air	149715.6	11.89	1780638.9	494.62
Outlet air (dry)	149573.8	18.09	2705784.2	751.61
Purge Outlet	141.7	75.24	6157.9	1.71

The energy efficiency of the Molseive is expressed by the equation (10) :

$$\eta = \frac{Q\ useful}{Q\ in} \qquad (10)$$

$$\eta = \frac{\text{H dry air+H purges}}{\text{H washed air}} = 79{,}86\ \%$$

The energy losses are expressed by the equation (11) :

Losses: $\Delta H = H_{\text{out, total}} - H_{\text{in, Total}}$ (11)

Losses =754.57−494.62 =259.95kW

Table 8 : Molseive Results Comparaison

	Stream	h [kJ/kg]	H [kJ/h]	Losses [KW]
Actual 'analysis'	Washed air	11.89	$1,78\times10^6$	259.95
	Pure air	18.09	$2,70\times10^6$	
	Purges	43.42	6.157×10^4	
Actual 'Aspen hysys'	Washed air	–31,51	$-4\ ,71\times10^6$	263,873
	Pure air	-13,33	$-1,99\times10^6$	
	Purges	$-1,25\times10^4$	$-1,77\times10^4$	

3.1.4 Heater E2618:

- Mass Balance:

mass is conserved, with identical inlet and outlet flow rates of 15128,2 kg/h, and no mass losses observed ($\dot{m}_{\text{losses}}$ = 0 kg/h)

- Energy balance:

$H_{\text{in}} = 1,057\times10^7$ kJ/h

$H_{\text{out}} = 1,383\times10^7$ kJ/h

$\Delta H = 1,383\times10^7 - 1,057\times10^7 = 3,257\times10^6$ kJ/h

useful energy absorbed by the gas is $3,257\times10^6$ kJ/h (Q_{useful} =904.96 kW)

The efficiency of the heater is expressed by the equation (12):

$$\eta = \frac{Q_{useful}}{Q_{electric}} \qquad (12)$$

$$\eta = 95\%$$

Where $Q_{electric}$ =952.58 KW From data sheet

- The losses are expressed by the equation (13) :

$$\text{Losses} = Q_{electric} - Q_{useful} \qquad (13)$$

$$\text{Losses} = 47{,}62 \text{ kw}$$

3.1.5 Expander-Booster C3420 / X3471:

- Mass balance

The mass balance is maintained (inlet flow rate equals outlet flow rate), with a value of 1.10755×10^5 Kg/h for the expander and 1.28019×10^5 Kg/h for the booster.

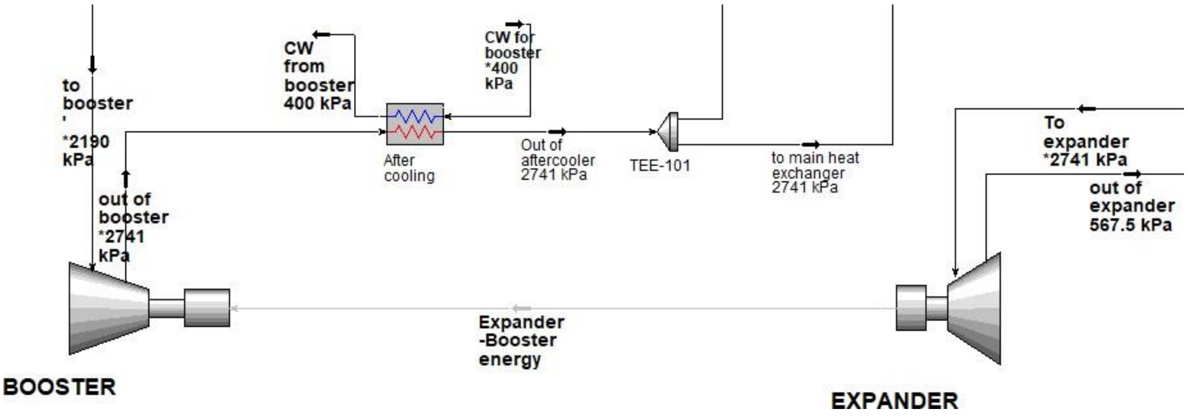

Figure 5: Configuration of the Booster - Expander in Aspen HYSYS

- Energy balance:

– Expander:

The enthalpy was calculated using the formula (14):

– $h = Cp \times T$ (14) [kJ/kg]

Inlet (135 K): $Cp = 0.947$ kJ/kg. K & Outlet (100 K): $Cp = 0.830$ kJ/kg. K

The expander power is calculated using the equation (15) :

$$W_{expander} \text{ (kJ/h)} = H_{in} - H_{out} \qquad (15)$$

The used specific heats are extracted from the data tables provided in Appendix.

- Booster:
  The enthalpy values were determined using the Mollier diagram (refer to the appendix)
  And the booster power is calculated using the equation (16)

$$W_{Booster}\ (kJ/h) = H_{out} - H_{in} \qquad (16)$$

Table 9 : Energy Balance Summary for the Expander

h_{in} (kJ/kg)	h_{out} [kJ/kg]	$W_{expander}$ [kJ/h]	$W_{expander}$ [kW]
88.85	119,94	3.444×10^{6}	957

Table 10 : Energy Balance Summary for the Booster

h_{in} (kJ/kg)	h_{out} (kJ/kg)	$W_{Booster}$ (kJ/h)	$W_{Booster}$ (kW)
292	315	2.939×10^{6}	816.57

Tables [11] and [12] present the energy losses and compare the theoretical results from the datasheet with the actual calculated and the results from Aspen hysys, in order to evaluate the losses associated with the booster and the expander individually. So, we calculate first their respective efficiencies using the formula (17) and (18) respectively:

$$\eta_{s,\ expander} = \frac{W\ actual}{W\ isentropic} = \frac{\dot{m}\ \times (h1 - h2)}{\dot{m}\ \times (h1 - h2S)} \qquad (17)$$

$$\eta_{s,\ booster} = \frac{W\ isentropic}{W\ actual} = \frac{\dot{m} \times (h2s - h1)}{\dot{m}\ \times (h2 - h1)} \qquad (18)$$

Table 11 : Theoretical vs. Actual Performance Data of the Expander

	Q [Nm^3/h]	T_{in} [K]	T_{out} [K]	P_{in} [Pa]$\times10^5$	P_{out} [Pa] $\times10^5$	W_{actual} [kw]	Wis [kw]	losses [kw]	ηs [%]
theoretical Data Sheets	84970	135	100	28,32	5.82	968.3	1120	151.7	86
Actual ‘analysis’	85737	134	100	28.04	5.76	957	1181.48	224.48	81
Actual Aspen hysys	85737	134	100	28.04	5.76	946.9	1183.62	236.72	80

Table 12 : Theoretical vs. Actual Performance Data of the Booster

	Q [Nm^3/h]	T_{in} [K]	T_{out} [K]	P_{in} [Pa]$\times10^5$	P_{out} [Pa] $\times10^5$	W_{actual} [kw]	Wis [kw]	losses [kw]	ηs [%]
theoretical Data Sheets	98110	290	313.3	22.10	28,60	956.3	692.47	263.83	82
Actual ‘analysis’	98490	290.97	313.8	21.90	27.41	816,57	653.25	163.32	80
Actual Aspen hysys	98490	290.97	313.8	21.90	27.41	831,38	681.72	149.65	82

Shaft losses (ΔW) between Expander and Booster is calculated using the equation (19):

$$\Delta W = W_{\text{expander}} - W_{\text{booster}} \quad (19)$$

$$= 946.9\text{-}831.38 = 115.52 \text{ kW}$$

$$\eta_{\text{loss}} = \frac{\Delta W}{W_{\text{expander}}} \times 100 = \left(\frac{115{,}52}{946{,}9}\right) \times 100 = 12.19\ \%$$

3.1.6 Pumps:

- Masse balance:

The mass balance is conserved for all pumps (inlet = outlet), with flow rates of 2.9262×10^4 kg/h for the LOX pump (P3568), 1.250×10^4 kg/h for the LIN pump (P3569), 5.0897×10^4 kg/h for the cooling water pump, and 5.0267×10^4 kg/h for the chilled water pump

- Energy balance

Table 13 : Energy Balance Summary for the pumps

Unit	H_{in} [kJ/h]	H_{out} [kJ/h]	W_{pump} [kJ/h]	W_{pump} [Kw]
LOX Pump	-1.152×10^7	-1.1411×10^7	1.0917×10^5	30.32
LIN Pump	-4.8481×10^6	-4.7889×10^6	5.9262×10^4	16.46
Cooling Water	-8.0792×10^8	-8.0790×10^8	1.4714×10^4	5.68
Chilled Water	-7.9989×10^8	-7.9975×10^8	1.348×10^5	37.45

In order to evaluate the losses associated with the pumps, we begin by calculating their respective efficiencies using the following formula (20)

$$\eta_{\text{hydraulic}} = \frac{\text{hydraulic power output}}{\text{power absorbed}} = \frac{\dot{m} \times g \times H}{\text{power absorbed}} \quad (20)$$

The losses are expressed by the equation (21)

$$\text{Losses} = P_{abs} - P_{hyd} \quad (21)$$

Tables [14] present the energy losses and compare the theoretical results from the datasheet with the actual calculated results for the pumps

Table 14 : Theoretical vs. Actual Performance Data of the pumps

Pump	Head [m]	Q [m³/s] ×10⁻³	Pabs [kW]	P_{hyd} [kW]	η_{hyd} [%]	Losses [kW]
Chilled Water P2467A/B	239.98	16.66	56.00	39.23	70	16.76
		14.00	49.48	37.92	67	16.52
Cooling Water P8466C/A	30.98	1.94	88.45	70.49	80	17.95
		6.11	110.09	71.75	65	38.33
LIN 3569A/B	351.00	4.83	35.04	16.64	47	18.39
		4.16	32.00	14.34	45	17.65

LOX P3568A	278.00	_	7.22 5.50	50.10 42.00	19.69 14.99	39 36	30.40 27.00

3.1.7 Main heat exchanger E3116:

The following figure (6) presents a simplified schematic of the main heat exchanger (E3116) in the Air Separation Unit (ASU).

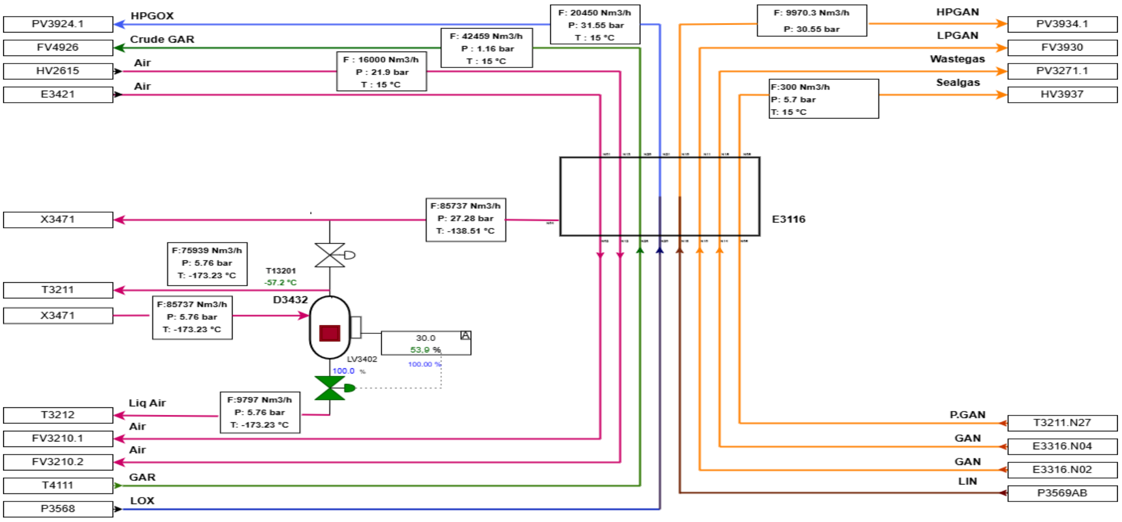

Figure 6 : Simplified schematic of the main heat exchanger (E3116) in the ASU

- Masse balance

The mass balance is conserved, with identical inlet and outlet flow rates of 326075,579 kg/h, and no mass losses observed ($\dot{m}_{losses}$ = 0 kg/h)

- Energy balance:

Table 15 : Energy Balance Summary for the Main Heat Exchanger

Stream	ṁ [Kg/h]	Cp in [kJ/kg. K]	H in [Kw]	Cp out [kJ/kg. K]	H out [kW]
1 – Air HV2615	39287,6241	1.004	9251.84	0.97	4014.61
2 – Air E3421	110285,682	1.004	2486.08	0.94	1041.26
3 – LOX	29517,3825	0.94	708.61	1.008	2463.76
4 – Seal Gas (1)	390,1580	0.99	10.57	1.005	32.47

5 – LIN	12507,4889	0.97	330.33	0.995	569.70
6 – Seal Gas (2)	12469,8170	0.93	312.96	1.003	1035.67
7 – Waste Gas	47600,2890	0.92	942.39	1.001	3720.51
8 – GAR	74017,1370	0.88	1701.29	1.003	5941.20

The Efficiency of the main heat exchanger is calculated using the equation (22) :

$$\varepsilon = \frac{Q_{real}}{Q_{max}} \qquad (22)$$

$$\varepsilon = \frac{T_{out}^{cold} - T_{in}^{cold}}{T_{hot\ in} - T_{Cold\ in}} = \frac{25-(-195{,}7)}{28-(-195{,}7)} = \frac{206{,}2}{209{,}2} = 0{,}98$$

Total losses are expressed using the equation (23)

$$Q_{total} = |Q_{lost} - Q_{gained}| \qquad (23)$$

Where:

$Q_{lost} = \sum_{i=1}^{8} |\Delta Hi| = -\sum_{i=1}^{2} \Delta Hi = 6682.05kW$

$Q_{gained} = \sum_{i=2}^{8} \Delta Hi = 9756.16Kw$

$Q_{gained} = |Q_{lost} - Q_{gained}| = 3074.11Kw$

- Comparing with Aspen Hysys we found that:

$Q_{lost=}$ 5929.22 Kw

$Q_{gained=}$ 9917.05 Kw

The total loss is 3987,82 kw

3.1.8 Distillation column:

In a distillation column, the energy balance is determined using the formula (24):

$$\sum H_{in} + Q_{reboiler} = \sum H_{out} + Q_{condenser} + losses \qquad (24)$$

- Masse balance

The mass balance is fully conserved in both the high- and low-pressure columns, with equal inlet and outlet flow rates of 137145.09 kg/h and 111619.79 kg/h, respectively.

- Energy balance

Table 16 : HP & LP Distillation Columns – Energy Balance Summary

Column	Stream	h [kJ/kg]	Q [kJ/h]	∑ΔH + Q	Losses [kJ/h]
HP	Air from MHE	-377.29	3.144×10^{6}	$-3{,}775\times10^{6}$	21,270
	Air from Expander	-205.36			
	N_2 Gas (outlet)	-216.73	1.591×10^{7}	-3.177×10^{7}	
	Liquid N_2	-387.62			
	Seal Gas	-380.77			
	Air (medium use)	-380.73			
	Liquid Air	-379.77			
LP	LP1 (inlet)	-197.47	2.085×10^{7}	-1.555×10^{7}	169.84
	LP2	-379.87			
	LP3	-379.19			
	LP4	-398.39			
	N_2 (outlet)	-227.02	2.750×10^{7}	-1.555×10^{7}	
	Waste Gas	-426.08			
	Oxygen	-387.03			

Chapter IV:

Results and discussion

Chapter IV: Results and discussion

Introduction:

The calculated results presented in this chapter are based on data obtained from thermodynamic tables provided in the appendix as well as the results of simulation carried out using Aspen HYSYS V11, accurately estimate the thermophysical properties of air components under cryogenic conditions. These sources provided the necessary thermophysical properties and process conditions required for accurate performance evaluation and analysis.

Table 17 : Thermophysical properties from Aspen HYSYS

Stream	Vap. Frac.	T (°C)	P (kPa)	$\dot{m}$ (kg/h)	H (kJ/h)
Air	1.0000	13.00	100.0	1.497e+05	-3.334e+06
Comp. Air 1	1.0000	83.91	182.0	1.497e+05	7.374e+06
Comp. Air 2	1.0000	98.57	331.0	1.497e+05	9.577e+06
Comp. Air 3	1.0000	96.10	602.0	1.497e+05	9.128e+06
Comp. Air 4	1.0000	98.34	1096	1.497e+05	9.347e+06
Comp. Air 5	1.0000	102.10	2066	1.497e+05	9.699e+06
To DCAC	1.0000	26.40	2215	1.497e+05	-2.174e+06
Washed Air	1.0000	10.90	2212	1.497e+05	-4.713e+06
CW to DCAC	0.0000	10.40	2455	5.027e+04	-7.998e+08
Purges	0.2752	18.00	2212	141.7	-1.779e+06
To Booster	1.0000	17.97	2190	1.280e+05	-1.703e+06
Out of Booster	1.0000	39.83	2741	1.280e+04	1.054e+06
To Expander	1.0000	-138.0	2471	1.108e+05	-2.180e+07
Out of Expander	0.9073	-173.4	567.5	1.108e+05	-2.456e+07
Liquid Air	0.0000	-174.3	580.0	9.633e+04	-3.658e+07
E4119	0.0000	-193.0	580.0	9.633e+04	-4.007e+07
To HP	0.0289	-175.2	570.0	3.929e+04	-1.482e+07
To HP Separator	1.0000	-173.4	567.5	9.786e+04	-2.010e+07
Air (HP)	0.0000	-174.7	574.4	390.2	-1.485e+05
LOX in Subcooler	0.0000	-182.7	120.0	2.203e+04	-8.527e+06
LOX Out	1.0000	25.00	3310	2.952e+04	-2.763e+04
LOX to MHE	0.0000	-181.2	3310	2.952e+04	-1.130e+07
LOX Tank	0.0000	-182.7	120.0	2.203e+04	-8.527e+06
OX	0.0000	-182.7	120.0	5.155e+04	-1.995e+07
LIN	1.0000	-177.2	570.0	2.753e+04	-5.966e+06
LIN Pump	0.0000	-177.2	570.0	1.251e+04	-4.848e+06
LIN Pump to MHE	0.0000	-175.1	3130	1.251e+04	-4.789e+06
LIN Out	1.0000	-108.4	3310	1.251e+04	-2.032e+06
LIN Out Subcooler	0.0000	-182.0	570.0	2.753e+04	-1.097e+07
LIN Sub	1.0000	-177.2	570.0	2.753e+04	-5.966e+06
Pure N_2	1.0000	-195.8	100.0	1.247e+04	-2.831e+06
Pure N_2 Out	1.0000	-176.0	100.0	1.247e+04	-2.577e+06
LP N_2	0.0000	-195.8	100.0	4.760e+04	-2.028e+07
Argon In	1.0000	-179.1	116.0	7.402e+04	-8.431e+06

Argon Out	1.0000	15.00	116.0	7.402e+04	-4.309e+05
Seal gas	0.0000	-174.7	574.4	390.2	-1.485e+05
Seal gas Out	1.0000	25.00	574.4	390.2	-625.7
LV3402	0.0000	-189.0	574.4	390.2	-1.596e+05
LP1	1.0000	-173.9	100.0	3.559e+04	-7.028e+06
LP3	0.1408	-195.8	100.0	2.753e+04	-1.097e+07
LP4	0.0293	-183.5	100.0	3.769e+04	-1.432e+07
To LP2	0.1816	-192.5	100.0	1.082e+04	-4.102e+06
Waste Gas	0.0000	-195.8	100.0	4.760e+04	-2.028e+07
Waste Gas Out Subcooler	0.8678	-195.7	100.0	4.760e+04	-1.204e+07
Waste Gas Out MHE	1.0000	25.00	100.0	1.247e+04	-3421
Pure N2 Out	1.0000	-176.0	100.0	1.247e+04	-2.577e+06

4.1 Calculation of the absolute humidity in the Main air compressor:

Saturation tables and a MATLAB code were used to determine the absolute humidity values based on the measured temperature and pressure conditions

It is assumed that the compression ratio ß is constant across all stages. This simplification ensures a uniform distribution of pressure increases.

This equation (25) allows the calculation of the inlet and the outlet pressures at each stage, with the results summarized in the table (18) .

$$ß = \left(\frac{P_{5'}}{P_1}\right)^{\frac{1}{5}} = \left(\frac{2056}{100.200}\right)^{\frac{1}{5}} = 1.83 \qquad (25)$$

$$ß = \frac{P_{1'}}{P_1} = \frac{P_{2'}}{P_2} = \frac{P_{3'}}{P_3} = \frac{P_{4'}}{P_4} = \frac{P_{5'}}{P_5} = 1.83$$

Table 18 : Pressure & Temperature conditions in each stage of The Main air compressor

	Stages	1	2	3	4	5
T[°C]	Inlet	13	25.6	24.6	27	27
	Outlet	83.91	98.6	96.1	98.34	102.1
P[kPa]	Inlet	100.200	183.366	335.5598	614.07439	1123.75615
	Outlet	183.366	335.5598	614.07439	1123.75615	2056

In order to evaluate the absolute Humidity at each compression stage**,** we use the Formula (4) :

Chapter IV: Results and discussion

The calculated inlet and outlet saturation pressures, as well as the absolute humidity at each stage, are summarized in the table (19)

Table 19 : Thermodynamic Parameters for Each Compressor Stage

	Stage	**1**	**2**	**3**	**4**	**5**
Inlet	T_{in}[°C]	13	25.6	24.6	27	27
	$P''_v(T_{in})$[kPa]	1.4979	3.2854	3.0954	3.567	3.567
	P_{in}[kPa]	100.200	183.366	335.5598	614.07439	1123.756
	X_{in}[kg/kg]	0.007719	0.11324	0.005791	0.0036342	0.001980
Outlet	T_{Out}[°C]	83.91	98.6	96.1	98.34	102.1
	$P''_v(T_{Out})$[kPa]	55.3909	96.3758	88.0137	95.4767	109.159
	P_{out}[kPa]	183.366	335.559	614.0743	1123.756	2056
	X_{Out}[kg/kg]	0.0077193	0.113242	0.005791	0.003634	0.00198

Observation:

Since the absolute humidity remains constant across each stage, no condensation occurs inside the compression stages themselves. Instead, condensation likely occurs between stages during intercooling, where the air is cooled and water vapor condenses out.

Result:

The total airflow rate entering the compressor is 115904 Nm³/h. This corresponds to the following:

$$\boldsymbol{m_{dry\ air}} = \frac{\boldsymbol{m_t}}{\boldsymbol{1+X}}$$

$$m_{dry\ air} = 149863.872 \text{kg/h}$$

$$L = m_{dry\ air} \times \Delta X_{1-5'} = 853.42 \text{kgH}_2\text{O /h}$$

4.2 Total losses:

Based on the energy balance results shown in Chapter 3 and the individual loss shown for each equipment in the ASU, we will calculate the total energy losses.

Table 20 : Total losses in the ASU

Equipment	Losses [Kw]
MAC	2011.72
DCAC	1.41
Molseive	263.87
Heater	47.62
Booster	149.65
Expander	236.72
Shaft booster – Expander	115.52
Pumps (LOX, Lin, Chilled water, Cooling water)	94.53
Main Heat Exchanger	3987,82
Distillation Column [(HP)+(LP)]	0.053
Total (Kw)	6861.30
Specific losses (kwh/Nm^3)	0.059

The total energy losses in the ASU unit are approximately 6861,3031 kW, which corresponds to a specific energy loss of 0,059 kWh/Nm^3.

4.3 The global mass balance:

The tables below provide a comparative analysis between the theoretical and actual values of the air inlet flow rate (expressed in Nm^3/h), as well as the liquid and gaseous product outputs (expressed in Nm^3/h). This comparison is established according to the required purity specifications of the final products.

- For oxygen:

Table 21 *: Theoretical vs. Actual Oxygen Production (Liquid and Gaseous [Nm³/h]) Based on Purity Requirements*

	Air Inlet Flow	O2 Inlet Flow	LOX	GOX	OX Total	purity	Net pure flow
Theoretical	115310	24157.4	1500	20450	21950	0,9995	21 840.250
Actual	95000	19902.5	2676.71	12452.9	15129.64	0.9995	15 053.998

- For nitrogen:

Table 22 : Theoretical vs. Actual Nitrogen Production (Liquid and Gaseous [Nm³/h]) Based on Purity Requirements

	Air Inlet Flow	O2 Inlet Flow	LIN	GAN	N2 Total	purity	Net pure flow
Theoretical	115310	90045.58	1500	9810	11310	0.9999	11308.86
Actual	95000	74185.5	585.125	9477.59	10062.70	0.9999	10061.70

The tables below provide a comparative analysis between the theoretical and actual values of the total net flow (expressed in Nm³/h) for both oxygen and nitrogen. This comparison aims to evaluate the total losses within the air separation unit.

Table 23 : Comparison Between Theoretical and Actual Total Net Flows [Nm³/h] of Oxygen and Nitrogen

	Total Net Flow	Loss flow Of Oxygen	%	Loss flow Of Nitrogen	%	Total Loss Flow	Losses [%]
Theoretical	33 149.119	2 317.195	9.592	78 736.710	87.44	81 053.90	70.2
Actual	25 115.700	4 848.502	24.361	64 123.798	86.43	68 972.3	72.6

The total actual mass loss of the unit is estimated at 68 972.3 Nm³/h, representing 72.602% of the actual total net flow. Theoretically, it is calculated to be 81053.90 Nm³/h, corresponding to 70.292% of the theoretical total net flow

4.4 Specific energy consumption:

The specific energy consumption is used as a Key Performance Indicator (KPI) for the selected Air Separation Unit (ASU) technologies. The specific energy consumption is determined using the following formula (26) [8]

$$\text{SEC} = \frac{\text{Net Energy Consumed (kwh)}}{\text{Total mass flow of products Kg/h}} \quad (26)$$

Net energy consumed is calculated using the formula (27):

$$W_{\text{total}} = \sum (E_{\text{compressors}} + E_{\text{Resistance}}) - \sum E_{\text{turbine}} \quad (27)$$

The following table (24) presents the energy consumption data for the Air Separation Unit (ASU), based on chapter 3 results.

Table 24 : The energy consumption data for the Air Separation Unit

Equipment	Power [kw]
Mac	13408 .4
Booster	831.38
Expander	946.9
Lox pump	30.33
Lin pump	16.46
Chilled water pump	37.45
Cooling water pump	4.087
Heater	831.39
Total [kw]	16106.397

Table 25 : Total mass flow of products Kg/h

Product	Flow rate [Nm^3/h]	ƒ [kg/Nm^3]	Flow rate [Kg/h]
LOX	2676.708	1.429	3823.0
GOX	12452.938	1.429	17778.7
LIN	585.125	1.251	731.6
GAN	9477.583	1.251	11859.6

- For Oxygen:

\- Total mass flow of oxygen = LOX + GOX

3823.0 kg/h+17778.7 kg/h=21601.7 kg/h which is equal to 21 512,163Kg/h at a 99,5% purity

- For Nitrogen

- Total mass flow of nitrogen = LIN + GAN

731.6 kg/h+11859.6 kg/h=12591.2 kg/h which is equal to 12587,18928 kg/h at a 99,9% purity

$\dot{m}_{\text{Total}} = \dot{m}_{\text{oxygen}} + \dot{m}_{\text{nitrogen}}$

= 21 512,163+12 587,18928 = 34 099,352 Kg/ h

$$\text{SEC} = \frac{\text{Net Energy Consumed (kw)}}{\text{Total mass flow of products Kg/h}} = \frac{16106{,}397}{34099{,}352} = 0{,}472\ \text{KWh/kg}$$

The energy consumption of the air separation unit is approximately 0.472 KWh/kg of total pure product.

For a pure oxygen flow rate of 21 512,163 kg/h at a purity of **99.5%**, the corresponding energy consumption is about 0,74 KWh/kg of total pure oxygen.

4.5 efficiency:

4.5.1 Separation efficiency:

The separation efficiency (η energy) is determined using the following formula (27) :

$$\eta\_{\text{Separation}} = \frac{\text{the total net pure flow of the products Nm3/h)}}{\textit{flow rate of the inlet air}\ \text{(Nm3/h)}} \times 100 \qquad (28)$$

the total net pure flow of the products is =net pure flow of oxygen + net pure flow of nitrogen depending on the table 4.9, the total net pure flow of the products is 25 115.700 Nm^3/h where the total flow rate of the inlet air is 115 904 Nm ^{3}/h

$$\eta_{\text{separation}} = \frac{25\ 115{,}700}{115\ 904} = 0{,}216693985 = 21.66\%$$

4.5.2 Overall efficiency:

The overall efficiency of the air separation unit is calculated using the formula (29) as the product of the efficiencies of the main components—MAC, booster, expander, and MHE—based on component-level results from Chapter 3 and following the methodology from Gürsoy et al. (2024).[6]

$$\eta_{\text{overall}} = \eta_{\text{MAC}} \times \eta_{\text{booster}} \times \eta_{\text{expander}} \times \eta_{\text{MHE}} \qquad (29)$$

$$=0,\ 85 \times 0.80 \times 0.81 \times 0.98 = 53\ \%$$

4.6 Discussion:

The results presented in this chapter provide a detailed assessment of the energy behavior of the Air Separation Unit. Based on the data and methods developed in Chapter 3, the analysis focuses on evaluating the performance of each component and identifying potential inefficiencies. In addition, the process simulation carried out using Aspen HYSYS was designed to operate under near-optimal conditions, allowing for the minimization of energy losses across each component. This approach provides a clearer picture of how energy is distributed and consumed within the system, offering insight into the unit's overall energy performance under idealized conditions.

Chapter IV: Results and discussion

The separation efficiency was determined to be 21.66%, which is consistent with the typical efficiency range of 18 to 25% for double-column cryogenic ASUs, as referenced by industrial case studies.

furthermore, the overall energy efficiency of the ASU based on the efficiencies of all the main components : main air compressor (MAC), booster, expander, and main heat exchanger (MHE) ,the resulting overall efficiency was 53%, which aligns with the documented range of 40.8% to 60% for large-scale cryogenic units under varying operational conditions.[6]

the Specific energy consumption (SEC) of the air separation unit (ASU) was calculated to be approximately 0.472 kWh/kg of total pure products. It is also calculated to be 0.74 kWh/kg for a pure oxygen production rate of 21 512.163 kg/h at 99.5% purity. When compared to the performance data reported by Alsultanny et al. (2014), which indicate that the specific energy consumption for conventional cryogenic ASUs ranges between 0.32 and 0.53 kWh/kg, the SEC value for total production falls into a reasonable and expected range. However, for pure oxygen (0.74 kWh/kg) is significantly higher than the average values reported in the same study. [9][8]

Thermal losses were identified as 6861.30 kW, which corresponds to 0.059 kWh/Nm^3 based on an inlet flow rate of 115904.7 Nm^3/h, closely matching the 0.050 kWh/Nm^3 loss reported by Kobe Steel (2015) for efficient double-column units. [10]

Gas losses were measured at 68972.3 Nm^3/h, or 72.6% of the actual total air flow of 95000 Nm^3/h (08-02-2025), which agrees with theoretical calculations (70.29% of theoretical net flow 115310 Nm^3/h). These losses primarily involve waste gas (crude Nitrogen) where its cold is recovered to cool the air in the main heat exchanger, water in the Evaporation cooler, it is also used as a seal gas and for the molecular sieves regeneration, which are characteristic of large-scale cryogenic systems. Argon recovery was not considered in this analysis due to its non-standard operation parameters.

General Conclusion

Conclusion

This final year project represents the only performance analysis of the Algerian Qatari steel' Air Separation Unit. The ASU's performance was evaluated using a combination of theoretical methods, Aspen HYSYS V11 simulation tools, and established engineering approaches methods. The study successfully produced a technically reliable and insightful analysis, despite facing major challenges due to limited access to actual plant data, mainly because of confidentiality policies.

The unit's separation efficiency was calculated to be 21.66%, which falls within the expected operational range for double-column ASUs while the overall energy efficiency of the ASU was calculated as 53% based on the efficiencies of all the main components which are the main air compressor (MAC), booster, expander, and main heat exchanger (MHE), which aligns with the documented range of 40.8% to 60% for large-scale cryogenic units under varying operational conditions.

In terms of energy performance, the specific energy consumption for total pure product was 0.472kWh/kg and 0.74kWh/kg for the 99.5% pure oxygen. Even if the overall energy consumption is within realistic ranges, the oxygen specific consumption is relatively high and there is still some space for performance improvement, in particular, at the compression and thermal integration levels.

The sum of the thermal losses of the plant was 6861.30kW, corresponding to 0.059kWh/Nm³ considering an inlet flow of 115904.7Nm³/h, which is a good thermal performance. Nevertheless, the gas wastes were extremely high of 68972.3Nm³/h or 72.6% of the incoming massive flow. This waste nitrogen is used as seal gas, for regenerating the molecular sieves, and for supplemental cooling. This is common in cryogenic equipment, such a high loss rate contributes to the relatively low separation efficiency.

The study successfully produced a technically dependable and insightful analysis. Importantly, the unit has not yet shown any major degradation on its performance, and the obtained results serve as proof that it is still working properly.

Even with incomplete data, the study was able to highlight key problems in process control, energy use, and gas management. These findings emphasize the importance of reliable data collection, accurate instrumentation, and continuous monitoring to support efficient plant operation. Based on the analysis, the following recommendations are proposed to improve the "ASU" performance:

- Optimize energy usage by integrating energy recovery systems and improving compressor operation.
- Upgrade control systems for more accurate and responsive process management.
- Reduce product and gas losses through improved sealing and column operation.

- Conduct regular performance and energy audits to identify inefficiencies and maintain optimal performance.
- Ensure better data access and monitoring to support technical analysis and process reliability.

In conclusion, this study demonstrates that simulation tools and engineering calculations can compensate for limited plant data to identify operational weaknesses and suggest targeted improvements. The work serves as a solid foundation for future optimization projects at the Bellara ASU and highlights the importance of precise data, sound technical methodology, and proactive maintenance in ensuring sustainable performance in industrial systems.

Bibliography

[1] A. R. Smith and J. Klosek, “A review of air separation technologies and their integration with energy conversion processes,” *Fuel Process. Technol.*, vol. 70, no. 2, pp. 115–134, 2001, doi: 10.1016/S0378-3820(01)00131-X.

[2] S. N. Sapali and V. N. Raibhole, “Exergy Analysis of Cryogenic Air Separation Unit Integrated with Biomass Gasifier,” no. October 2013, 2017.

[3] L. Kumar, “Analysis of steady state Cryogenic Air Separation unit of Rourkela Steel Plant and simulation of Fixed Bed Adsorption Separation of Air Analysis of steady state Cryogenic Air Separation unit of Rourkela Steel Plant and simulation of Fixed Bed Adsorption S,” no. June, 2014.

[4] E. Saving, I. N. Cryogenic, A. I. R. Separation, P. Applying, and H. R. Technology, “ICMERE2015-PI-023 ENERGY SAVING IN CRYOGENIC AIR SEPARATION PROCESS APPLYING SELF,” vol. 2015, pp. 26–29, 2015.

[5] S. Bucsa *et al.*, “Exergetic Analysis of a Cryogenic Air Separation Unit,” 2022.

[6] E. Gürsoy, E. Gedik, A. G. Georgiev, A. Keçebaş, and H. Kurt, “Performance improvement of air separation unit for an iron - steel industry using enhanced exergy analysis,” *J. Therm. Anal. Calorim.*, vol. 149, no. 8, pp. 3259–3266, 2024, doi: 10.1007/s10973-024-12921-2.

[7] S. Cooling Technologies, “Effects of Relative Humidity-Thermal Performance,” 2018, [Online]. Available: www.linric.com

[8] A. Lawrence, P. Thollander, M. Andrei, and M. Karlsson, “Specific energy consumption/use (SEC) in energy management for improving energy efficiency in industry: Meaning, usage and differences,” *Energies*, vol. 12, no. 2, 2019, doi: 10.3390/en12020247.

[9] Y. A. Alsultanny and N. N. Al-Shammari, “Oxygen specific power consumption comparison for air separation units,” *Eng. J.*, vol. 18, no. 2, pp. 67–80, 2014, doi: 10.4186/ej.2014.18.2.67.

[10] M. Taniguchi, H. Asaoka, and T. Ayuhara, “Energy saving air separation plant based on exergy analysis,” *R D Res. Dev. Kobe Steel Eng. Reports*, vol. 64, no. 1, pp. 45–48, 2014.

- https://www.aiche-cep.com/cepmagazine/june_2020/MobilePagedArticle.action?articleId=1591898
- https://doi.org/10.1016/j.eneco.2015.08.023

Appendix

A/ Tables:

Thermodynamic tables were used to:

- determine the saturated pressure of the components involved in the air separation process:
- ➢ **https://www.thermopedia.com/content/1150/**
- Determine the specific heat capacity (Cp) of the cryogenic streams:
- ➢ **NIST WebBook – Air Data**

- For the MAC:

$$L_{v,\ effective}=Lv+C_{pv}\ (T_{in})\ (Lv = 2500\ kJ/kg\ when\ T = 0°C)$$

Table Appendix A.1: Lv values in the Main air compressor

Stage	T_{in}(K)	$L_{v,\ effective}$ (kJ/kg)
1	286.15	2500 + 1.84 × 286.15 = 3026.5
2	298.75	2500 + 1.84 × 298.75 = 3050.7
3	297.75	2500 + 1.84 × 297.75 = 3048.9
4	300.15	2500 + 1.84 × 300.15 = 3053.3
5	300.15	2500 + 1.84 × 300.15 = 3053.3

B/ Diagrams :

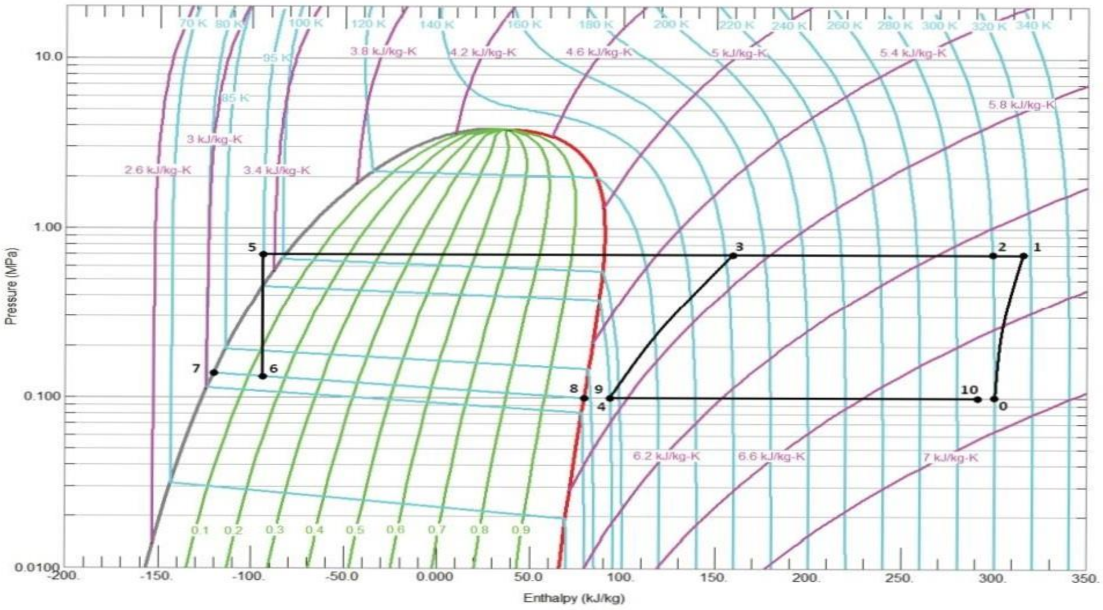

Appendix B.1: Pressure- enthalpy diagram of air.

C/ Drawings Based on the Distributed Control System (DCS) Interface of the Cryogenic Air Separation Unit:

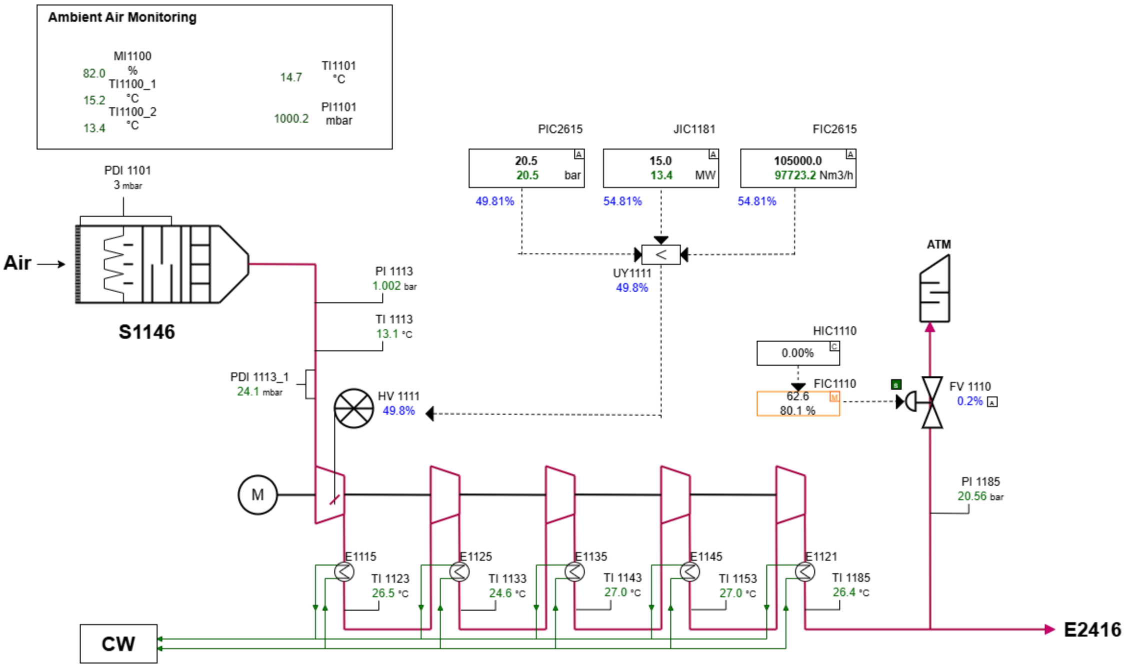

Appendix C.1: Simplified schematic of the Main air compressor column in the ASU

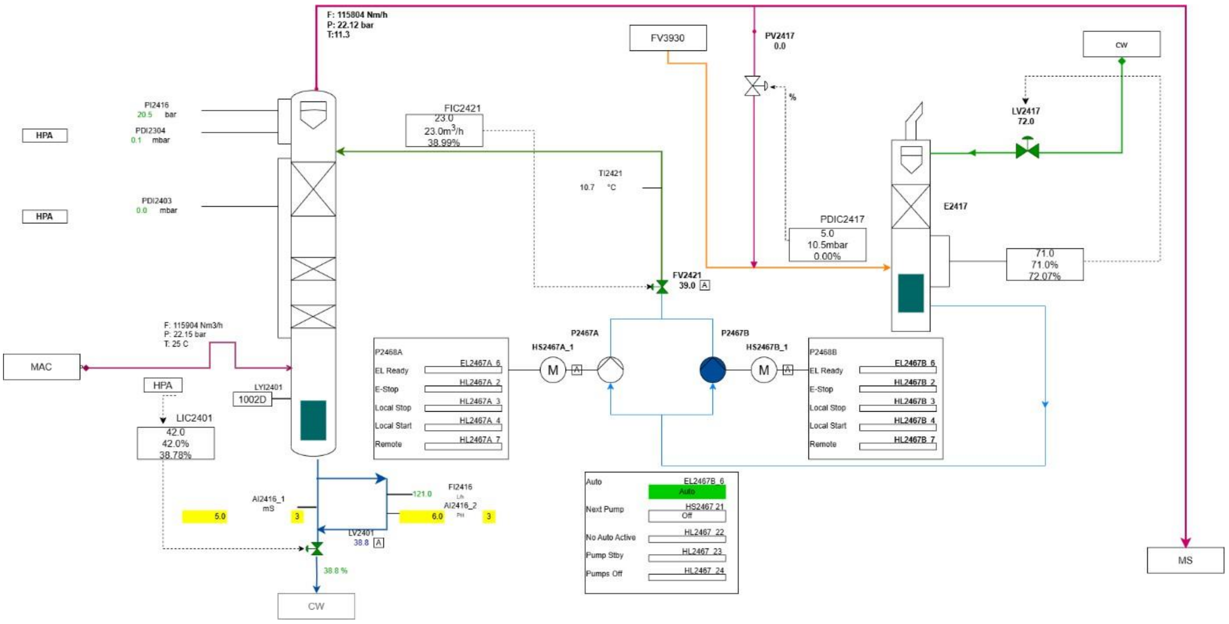

Appendix C.2: Simplified schematic of the DCAC in the ASU

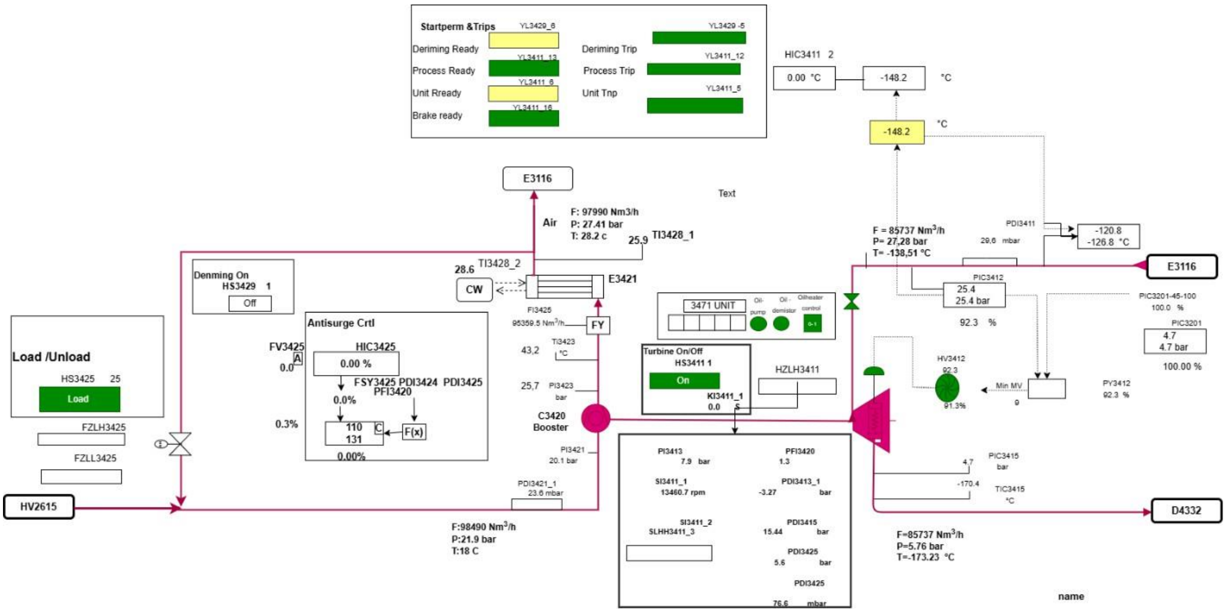

Appendix C.3: Simplified schematic of the Expander - Booster

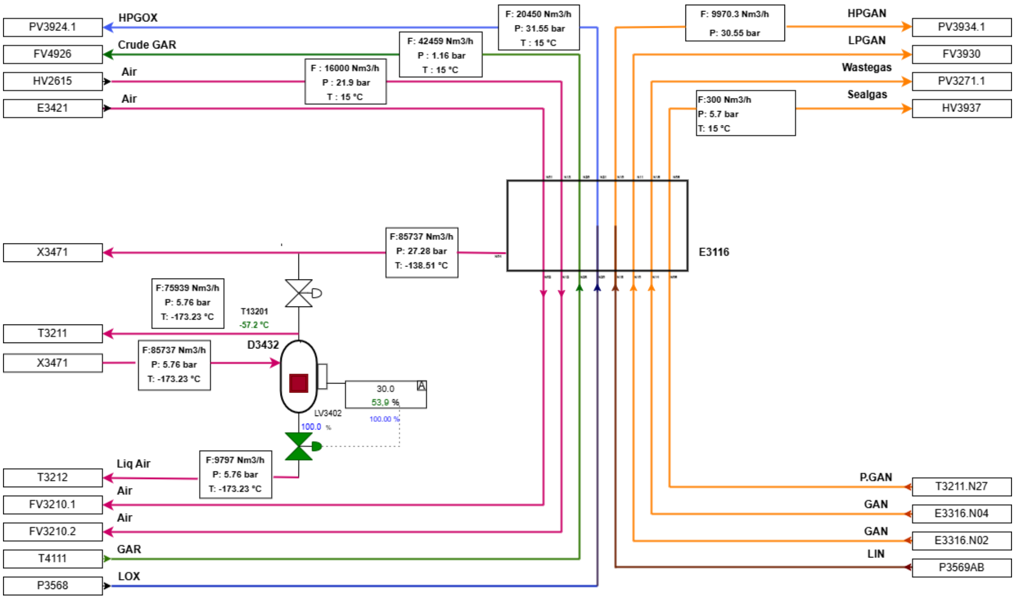

Appendix C.4: Simplified schematic of the Main heat exchanger in the ASU.

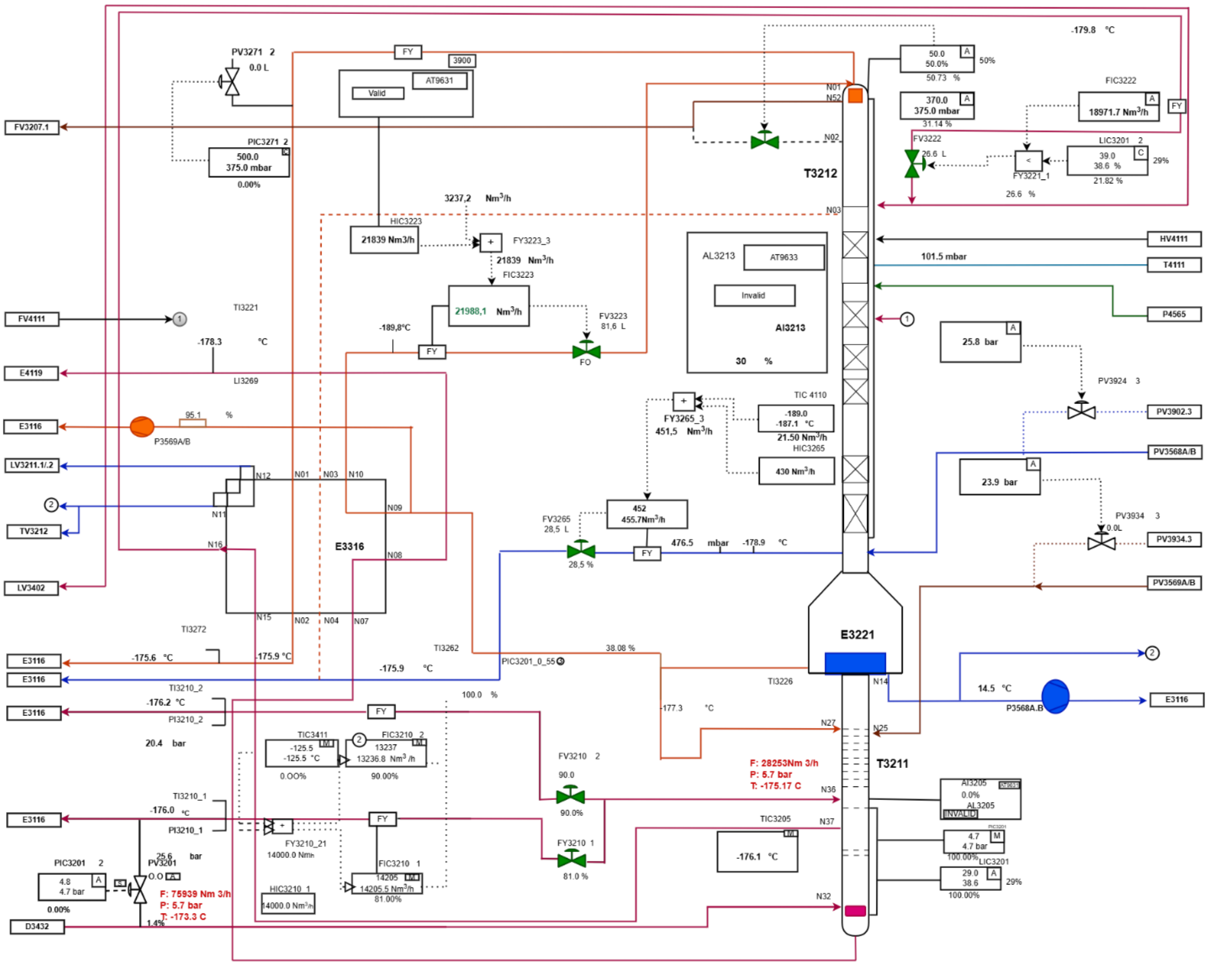

Appendix C.5: Simplified schematic of the distillation column in the ASU

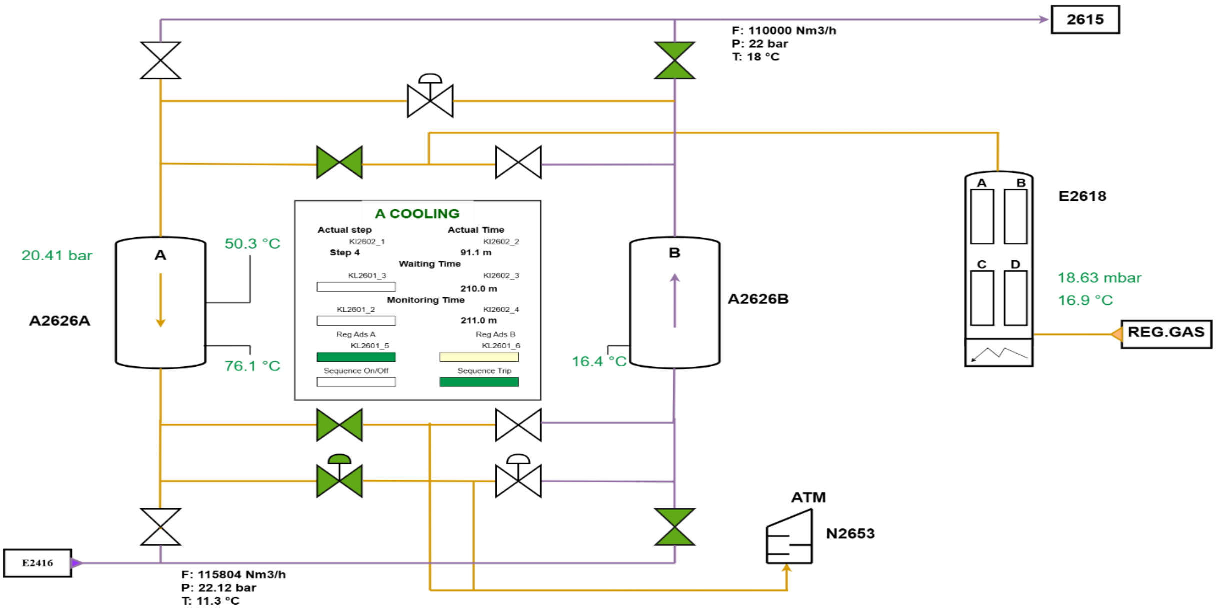

Appendix C.6: Simplified schematic of the Molseive in the ASU

D/ Real Images of the Cryogenic Air Separation Unit:

Appendix D.1: Real picture of the Molseive in the ASU

Appendix D.2: Real picture of the DCAC

Appendix D.3: Real picture of the Main AIR Compressor

Appendix D.4: real picture of the expander - Booster in the ASU

Appendix D.5: Real Picture of the main Heat exchanger

Appendix D.6: Real Picture impure Nitrogen Drain

Appendix D.7: Real picture of the distillation column

Appendix D.8: Real picture of the evaporation cooler

Appendix D.9: Real picture of air filter

Appendix D. 10: Real picture of the silencer

Appendix D.11: Cooling water pumps

Appendix D.12: Chilled water pumps